Ovary ecdysteroidogenic hormone functions independently of the insulin receptor in the yellow fever mosquito, *Aedes aegypti*

Animesh Dhara [a,b], Jai-Hoon Eum [a], Anne Robertson [a], Monika Gulia-Nuss [a,c], Kevin J. Vogel [a], Kevin D. Clark [a,b,c,d], Rolf Graf [d], Mark R. Brown [a,*], Michael R. Strand [a,*]

[a] *Department of Entomology, University of Georgia, Athens, GA 30602, USA*
[b] *Department of Microbiology, Immunology, and Molecular Genetics, University of Kentucky College of Medicine, Lexington, KY 40536, USA*
[c] *Department of Entomology, Purdue University, West Lafayette, IN 47907, USA*
[d] *Pancreatitis Research Laboratory DL 34, Rämistrasse 100, Universitätsspital Zürich, 8091 Zürich, Switzerland*

ABSTRACT

Most mosquito species must feed on the blood of a vertebrate host to produce eggs. In the yellow fever mosquito, *Aedes aegypti*, blood feeding triggers medial neurosecretory cells in the brain to release insulin-like peptides (ILPs) and ovary ecdysteroidogenic hormone (OEH). Theses hormones thereafter directly induce the ovaries to produce ecdysteroid hormone (ECD), which activates the synthesis of yolk proteins in the fat body for uptake by oocytes. ILP3 stimulates ECD production by binding to the mosquito insulin receptor (MIR). In contrast, little is known about the mode of action of OEH, which is a member of a neuropeptide family called neuroparsin. Here we report that OEH is the only neuroparsin family member present in the *Ae. aegypti* genome and that other mosquitoes also encode only one neuroparsin gene. Immunoblotting experiments suggested that the full-length form of the peptide, which we call long OEH (lOEH), is processed into short OEH (sOEH). The importance of processing, however, remained unclear because a recombinant form of lOEH (rlOEH) and synthetic sOEH exhibited very similar biological activity. A series of experiments indicated that neither rlOEH nor sOEH bound to ILP3 or the MIR. Signaling studies further showed that ILP3 activated the MIR but rlOEH did not, yet both neuropeptides activated Akt, which is a marker for insulin pathway signaling. Our results also indicated that activation of TOR signaling in the ovaries required co-stimulation by amino acids and either ILP3 or rlOEH. Overall, we conclude that OEH activates the insulin signaling pathway independently of the MIR, and that insulin and TOR signaling in the ovaries is coupled.

© 2013 Elsevier Ltd. All rights reserved.

1. Introduction

A key feature of mosquito biology is that most species must feed on the blood of a vertebrate host to produce a clutch of eggs. The physiological and molecular events regulating egg production in mosquitoes are best understood in the yellow fever mosquito, *Aedes aegypti*, which is a major vector of pathogens that cause several human diseases. After adult eclosion, *Ae. aegypti* females enter a pre-vitellogenic phase where juvenile hormone III from the corpora allata (CA) programs reproductive competency by stimulating the expression of target of rapamycin (TOR) and ecdysteroid hormone signaling pathway components in the fat body, midgut, and ovaries (Hansen et al., 2004; Zhu et al., 2003, 2006; Clifton and Noriega, 2011; Perez-Hedo et al., 2013; Zou et al., 2013). Oogenesis thereafter remains arrested until a female consumes a blood meal, which triggers neurosecretory cells in the brain to release two types of neuropeptide hormones: ovary ecdysteroidogenic hormone (OEH) and insulin-like peptides (ILPs) (Brown et al., 1998; Riehle et al., 2006). OEH and ILPs stimulate the ovaries to produce ecdysteroid hormone (ECD) (Brown et al., 1998, 2008; Wen et al., 2010), while ILPs together with amino acid sensing through the TOR pathway induce the midgut to produce serine proteases that digest the blood meal. The interaction of ILPs, OEH, ECD, and TOR stimulate the fat body to produce yolk proteins from teneral reserves and blood meal-derived amino acids, which are then taken up by the ovaries and packaged into oocytes (Attardo et al., 2005; Hansen et al., 2005; Roy et al., 2007; Bryant et al., 2010; Roy and Raikhel, 2011; Gulia-Nuss et al., 2011). Yolk packaging and chorion formation are completed by 36 h post-blood meal (PBM) followed by oviposition of 120–150 eggs by 72 h.

* Corresponding authors. Tel.: +1 706 542 2816; fax: +1 706 542 2279.
E-mail addresses: mrbrown@uga.edu (M.R. Brown), mrstrand@uga.edu (M.R. Strand).

Most insects, including mosquitoes, encode multiple ILPs but only one receptor tyrosine kinase (RTK) homolog of the mammalian insulin receptor (IR) (Wu and Brown, 2006; Baker and Thummel, 2007; Antonova et al., 2012). Prior studies with *Ae. aegypti* show that ILP3 stimulates the ovaries to produce ECD by binding with high affinity to the mosquito insulin receptor (MIR) (Brown et al., 2008; Wen et al., 2010; Gulia-Nuss et al., 2011). In contrast, much less is known about the function of OEH, which is a member of an understudied neuropeptide family in arthropods called neuroparsins (Badisco et al., 2007; Veenstra, 2010). In *Ae. aegypti,* the OEH gene produces a predicted 149 amino acid pre-propeptide that after signal peptide removal yields a 13.7 kDa propeptide (residues 23-149) we refer to as the long form of OEH (lOEH). In contrast, purification of OEH from adult females identified an 8.8 kDa C-terminal truncation of lOEH (residues 23-108) that we call short OEH (sOEH) (Brown et al., 1998). It is unknown whether a specific protease cleaves lOEH to produce sOEH or if lOEH and sOEH differ in biological activity.

Also unknown is the mode of action of OEH. No receptor has been identified for any neuroparsin family member, but it was suggested that neuroparsins share features with the amino (N)-terminal domain of vertebrate insulin-like growth factor binding proteins (IGFBPs), which bind to insulin-like growth factors (IGFs) (Badisco et al., 2007; Rosenweig and Atreya, 2010). Since IGFs and insulin are structurally similar hormones, this led to the hypothesis that neuroparsins function by binding to ILPs (Badisco et al., 2007, 2008). Alternatively, OEH could function independently of ILPs and activation of the MIR.

In the first part of this study, we examined structural features of OEH from *Ae. aegypti* and compared the biological activity of lOEH to sOEH and ILP3. We then conducted studies that characterized OEH signaling activity in ovaries. We found that hemolymph predominantly contains sOEH, but lOEH and sOEH exhibit very similar biological activity. We also report that OEH does not bind to ILP3 or the MIR but it stimulates phosphorylation of Akt, which is a key regulatory nexus of insulin signaling.

2. Materials and methods

2.1. Mosquitoes

The UGAL strain of *Ae. aegypti* was used in all experiments. All stages were maintained at 27 °C in a 16 h light/8 h dark photoperiod, and larvae were fed a standard diet (Brown et al., 2007). Adults were provided water continuously but were fed a 5% sucrose solution on day 2 post-eclosion. Females obtained blood meals from anesthetized rats (UGA Animal Use Protocol A2010-6-094). This protocol was reviewed and approved by The University of Georgia Institutional Animal Care and Use Committee (IACUC) who oversees and provides veterinary care for all campus animal care facilities. IACUC is accredited by the Association for Assessment and Accreditation of Laboratory Animal Care International (AAALAC), is licensed by the US Department of Agriculture, and maintains an Assurance of Compliance with the US Public Health Service.

2.2. Alignments

Homologous genes to OEH were identified from *Ae. aegypti*, select other mosquitoes with sequenced genomes (*Anopheles gambiae*, *Culex quinquefasciatus*), and select species in the genus *Drosophila* using blastx and the NCBI nonredundant database. Identified neuroparsin family members from these dipterans plus neuroparsin A from the orthopteran *Locusta migratoria*, neuroparsin 1 from *Schistocerca gregaria*, and human IGFBP7 were then downloaded and aligned using MAFFT (Katoh et al., 2005) followed by manual editing in Mesquite.

2.3. sOEH, lOEH, and ILP3

sOEH was synthesized using Fmoc chemistry and a Perkin Elmer ABI433 peptide synthesizer (Stefan Klauser, University of Zürich). To prevent possible formation of diketopiperazine and premature termination of the synthesis, sterically hindered H–Arg(Pmc)–2ClTrt-resin (Novabiochem, Switzerland) was used as the solid phase support (Barlos et al., 1989, 1993). Side chain functional groups were protected as follows: Arg(Pmc), Asn(Trt), Asp(OtBu), Cys(Trt), Gln(Trt), Glu(OtBu), His(Trt), Lys(Boc), Ser(tBu), Thr(tBu) and Tyr(tBu). Progress of the synthesis was verified at different cycles by mass spectrometry and finally terminated by coupling the N-terminal pGlu. After washing with dichloromethane and methanol, the peptidyl-resin was dried and then cleaved by incubation in a mixture of 90% trifluoroacetic acid, 2.5% water, 2.5% ethanedithiol, and 5% thioanisole for 2 h at room temperature (RT). The crude peptide was twice precipitated in ice-cold t–butylmethylether and pelleted by centrifugation (4 C, 15 min), dried under a stream of nitrogen, and stored at −20 °C. After purification on a preparative reverse phase (RP) HPLC column, peptide fraction aliquots were checked for bioactivity in the *in vivo* assay (see below). Fractions containing bioactive peptide were pooled and lyophilized for an additional step to enhance bioactivity. The peptide (∼10 mg) was dissolved by stirring in 1 ml of denaturing buffer (25 mM Tris pH 8.0, 5 M urea, and 5 mM EDTA), and over 2 h, 2.5 volumes of the oxidizing/reducing solution (25 mM Tris, pH 8.0, 5 mM EDTA, 8 mM reduced glutathione, 4 mM oxidized glutathione; SIGMA) were added (Han et al., 1997; Hsih et al., 1997). The reaction was allowed to equilibrate for one day at RT, and then the oxidized peptide was checked by electrospray mass analysis, dialyzed (10 mM Tris pH 8.0, 0.1 M NaCl), and lyophilized. This peptide was then purified on a C18 column by HPLC (Jupiter 5 μM, 300 A, C18). Fractions containing the peptide were pooled and lyophilized, so that sOEH could be weighed, solubilized in water as a 200 μM stock, aliquoted for use in bioassays, and stored at −80 °C.

Full-length OEH was produced in *Escherichia coli* as previously described (Gulia-Nuss et al., 2012). In brief, OEH was PCR amplified using OEH specific primers and cDNA as template followed by cloning into pET-32 (Novagen) to produce an OEH-thioredoxin fusion protein (30.5 kDa). Enterokinase (EMD Millipore) was used to cleave the fusion tag, which resulted in full-length OEH with an N-terminal His tag (18.3 kDa) that we named rlOEH. This product was then quantified after Ni-affinity purification and diluted to a 200 μM stock that was stored at −80 °C until use in bioassays. ILP3 and ILP4 were synthesized as previously described (Brown et al., 2008).

Purified rlOEH or sOEH together with protein samples from heads of non-blood fed females or hemolymph collected from females at 24 h PBM were collected in lysis buffer (Gulia-Nuss et al., 2012), electrophoresed on 16.5% Tris-tricine gels (BioRad) under reducing conditions, and transferred to nitrocellulose (Protran 0.1 μm, GE Healthcare) in Tris-glycine/20% methanol buffer. After blocking, membranes were incubated overnight (4 °C) with a previously generated OEH antibody (Brown and Cao, 2001) at a dilution of 1:10,000 in Tris buffered saline plus 0.1% Tween 20) followed by visualization using a peroxidase-conjugated goat anti-rabbit secondary antibody (1:20,000; Sigma A6667), a chemiluminescent substrate (ECL Advance kit, GE Healthcare), the Gel Logic 4000 PRO platform (Carestream Health Inc, Rochester, NY).

2.4. In vivo assay for stimulation of yolk uptake into oocytes

Prior studies established that decapitation shortly after blood feeding blocks egg maturation as measured by yolk protein (YP) deposition into oocytes, while injection of sOEH or ILP3 dose-dependently rescues this response (Matsumoto et al., 1989;

Brown et al., 1998, 2008). We thus decapitated 3–5 day old females 1 h PBM, followed by injection of rlOEH, sOEH or ILP3 in 0.5 μl saline over a standard concentration range. Intact blood-fed females injected with saline served as a positive control while decapitated females injected with saline served as the negative control. At 24 h and 48 h PBM, ovaries were dissected and yolk deposition in oocytes measured along the anterior–posterior axis as previously described (Brown et al., 2008). A minimum of 4 females per dose was analyzed by measuring the average length of 10 oocytes per ovary pair for each female; at least 4 females per dose for each of 3 female cohorts.

2.5. In vitro assay for stimulation of ovary ecdysteroid production

Ovary ECD production was determined using a well-established in vitro assay (Sieglaff et al., 2005). Ovaries from non-blood fed females (two pairs per 60 μl, 6 h, 27 °C) were incubated alone or with the l or sOEH over a standard concentration range in a buffered saline (BS) or Sf-900 medium, which is a commercially available insect cell culture medium (Invitrogen) that contains all essential amino acids (Gulia-Nuss et al., 2011). At least three samples for each peptide concentration were included in each experiment with one of three female cohorts. In subsequent experiments, a predetermined amount of the TOR pathway inhibitor rapamycin (100 pmol/60 μl; LC laboratories, Woburn, MA) was added to medium as previously described (Wen et al., 2010). To some assays we also added 5 nmol/60 μl of PQIP (cis-3-[3-(4-methyl-piperazin-l-yl)-cyclobutyl]-1-(2-phenyl-quinolin-7-yl)-imidazo[1,5-a]pyrazin-8-ylamine) (OSI Pharmaceuticals, New York, NY), which is a potent and specific inhibitor that blocks ligand induced activation of the mammalian IR and insulin-like growth factor 1 receptor (IGFR-1) (Ji et al., 2007; Flanigan et al., 2010). Following incubation, medium (50 μl) from each sample and treatment was stored at −80 °C, followed by determination of ECD titers by radioimmunoassay (RIA) using an ecdysteroid antiserum (4919; ecdysone and 20-hydroxyecdysone equally recognized) kindly donated by P. Porcheron (Université P. et M. Curie, Paris France).

2.6. OEH-ILP3 binding assays

We assessed whether rlOEH or sOEH bound ILP3 by conducting immunoprecipitation and cross-linking experiments. Immunoprecipitation assays were conducted by adding equimolar amounts (70 pmol) of OEH and ILP3 alone (control) or together in buffered saline (1 ml) for 2 h at 4 °C, followed by addition of a previously generated OEH antibody and ILP3 antibody which were both generated in rabbits (2 μl neat; 30 °C) (Gulia-Nuss et al., 2012) for an additional 4 h. Washed and resuspended Protein A PLUS agarose (Santa Cruz Biotechnology) was the added (50 μl) to each sample and incubated overnight at 4 °C. After centrifugation, washing with the buffered saline and removal of the supernatant 2×, the agarose matrix was resuspended in 0.2 M HCl-glycine buffer with 0.1% Tween (25 μl). After centrifugation, the supernatant was immunoblotted and visualized as described above.

Cross-linking experiments were performed as outlined by Wen et al. (2010). Briefly, ^{125}I-ILP3 was labeled by the lactoperoxidase-hydrogen peroxide method. We then added rlOEH or sOEH (1 μg) and ^{125}I-ILP3 (20,000 cpms) alone (control) or together in buffered saline (40 μl total) and incubated overnight at 4 °C. Freshly prepared cross-linking reagents, Bis[sulfosuccin-imidyl] suberate and Bis[sulfosuccin-imidyl] glutarate (Aculytix, Rockford IL), were added to achieve a 100 μM final concentration. Sample tubes were placed on a rotator for 1 h at 4 °C followed by addition of Tris-tricine SDS sample buffer. The samples were electrophoresed and blotted. OEH was detected as described above while ^{125}I-ILP3-

protein conjugates were visualized by exposing blots to X-ray film (Kodak XR) for up to three weeks.

2.7. OEH-MIR binding assays

sOEH was labeled with [125]Iodine (Perkin–Elmer) using the lactoperoxidase-hydrogen peroxide or chloramine T method and purified by HPLC (Crim et al., 2002; Wen et al., 2010). Ovary membrane extracts were prepared using 300 ovary pairs collected from 4 to 7 day old non-blood fed adult females as previously described (Wen et al., 2010). Total binding was determined by incubating ^{125}I-sOEH (∼100–200 pM, ∼400 K cpm/150 μl) with ovary membranes (20 ovary pair equivalents in 20 μl) in binding buffer (50 mM HEPES (pH 7.6), 1× Hanks balanced salt solution, 3% BSA and 0.1× Roche protease inhibitors; 300 μl total volume) in 1.5 ml polypropylene microtubes. Unlabeled sOEH or rlOEH at 1–10 μM were added to samples (triplicate tubes/concentration) set up as above to compete with binding of the labeled sOEH. Samples were rotated overnight at 4 °C, centrifuged, and the supernatants removed by aspiration. The pelleted membranes were then rinsed with ice-cold binding buffer, re-centrifuged, and the supernatant again removed. Counts per minute were obtained for the sample pellets and converted to percent binding.

2.8. Insulin and TOR pathway activation assays

Twenty ovary pairs from non-blood fed females were dissected in ice-cold saline containing 1× protease inhibitor cocktail (Roche) and transferred to a microtube cap (1.5 ml) containing 100 μl of Sf-900 or buffered saline with 1× Halt protease and phosphatase inhibitor (PPI) cocktail (Thermo Scientific). rlOEH or ILP3 (40 pmol/20 μl) was then added to the ovaries alone or with rapamycin (200 pmol) or PQIP (10 nmol) for 30 min, 27 °C. After incubation, each cap was clipped onto a microtube and centrifuged to pellet the ovaries (1000 × g, 1 min, 4 °C). Supernatant was replaced with 100 μl of ice-cold immunoprecipitation lysis buffer (Pierce 87788) containing 1× PPI. After 5 min on ice, the ovary sample was homogenized (30–60 s), and another 100 μl of the above buffer was added to rinse the pestle. The ovary extract was freeze-thawed 3×, vortexed, sonicated with a probe set for brief, low pulses, and transferred to a 100 K MW cut-off column (Pall Life Sciences, Ann Arbor, MI). After centrifugation (13,000 × g, ∼40 min, 4 °C), the retentate (∼20 μl) and filtrate (∼180 μl) were collected separately and stored at −80 °C, and the protein content of each extract was determined (Bradford Coomassie kit, Thermo scientific, cat # 23200).

Aliquots (120 μg protein/well) of retentate or filtrate were mixed with Laemmeli sample buffer (non-reducing), heated at 90 °C for 5 min, and centrifuged, prior to loading onto a 4–20% Tris-glycine gel (BioRad Criterion) for separation (100 V, 4 °C) and transfer to nitrocellulose (Protran 0.2 μm, Whatman; 3 h at 50 V, 4 °C in 12 mM Tris-base, 96 mM glycine, 50% MeOH). After transfer, the membrane was dried, rewet in Tris buffered saline, treated with blocking agent (0.1 g/10 ml, GE Healthcare Advance kit), and incubated overnight (4 °C) with primary antibody added to the blocking buffer. The unphosphorylated form of the MIR was detected using a previously developed rabbit antibody (β chain specific 376, 1:6000). An anti-phosphotyrosine antibody was used to detect phosphorylated MIR (Invitrogen 61-5800, 1:1000) (Wen et al., 2010). We also used antibodies previously shown to specifically recognize phosphorylated Drosophila Akt kinase (p-Akt) (Ser505; Cell Signaling Technology (CST) 4054, 1:1000) and phosphorylated p70 S6 kinase (p-S6K) (Thr389; CST 9209, 1:1000) mediated through TORC1 in mammals and Drosophila melanogaster (Magnuson et al., 2012; Pallares-Cartes et al., 2012). An antibody to actin (CST 8456)
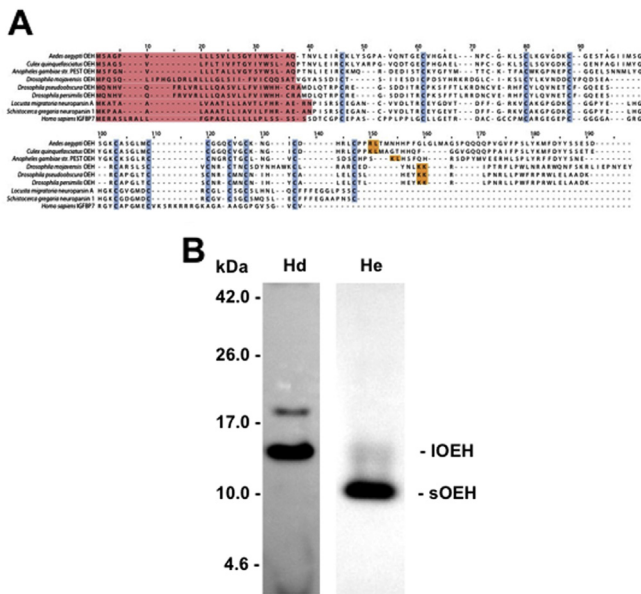
Fig. 1. (A) Sequence alignment of neuroparsins from select mosquitoes, drosophilids and orthopterans with the N-terminal domain of IGFBP7 from humans. Predicted signal peptides are highlighted in red while conserved cysteine residues are shown in blue. The arginine–leucine residues (R–L) where lOEH is processed to form sOEH in *Ae. aegypti* is indicated in yellow. Similarly positioned mono- or dibasic residues in the neuroparsins of other species are also highlighted in yellow. The sequences shown have the following GenBank accession numbers: *Ae. aegypti* (AAC38958), *An. gambiae* (XP_311039), *C. quinquefasciatus* (XP_001870999), *D. mojavensis* (XP_002000502), *D. pseudoobscura* (AADE01000437), *D. persimilis* (XP_002000502), *L. migratoria* neuroparsin A (P10776), *S. gregaria* neuroparsin 1 (CAC38869). (B) Head extracts from adult female *Ae. aegypti* (non-blood fed) predominantly contains lOEH while hemolymph (24 h PBM) predominantly contains sOEH. Representative immunoblot shows head extract (Hd) and hemolymph (He). Molecular mass markers are indicated to the left. Note that the bands corresponding to lOEH and sOEH run slightly higher when separated on a Tris-tricine gel than their predicted masses of 13.7 (lOEH) and 8.8 kDa (sOEH). The weak band in head extract that runs above the 17.0 kDa marker recognized by anti-OEH is the putative pre-proOEH. (For interpretation of the references to color in this figure legend, the reader is referred to the web version of this article.)

served as a loading control. All blots were visualized as described above. To observe the status of different signaling proteins, the same blot was stripped (0.2 M glycine, pH 2.5, 0.05% Tween 20, and 0.5% β mercaptoethanol; 60 °C, 1 h), washed extensively, dried, and treated with a different primary antibody, up to six times as above. Each immunoblotting experiment and treatment was also repeated a minimum of three times using independently prepared samples of ovary extracts.

2.9. Data analysis

All analyses were conducted using the JMP 10.0 statistical platform (SAS, Cary, NC, USA). Yolk deposition into oocytes and ECD production by ovaries were analyzed by ANOVA followed by the Dunnett's or Tukey–Kramer multiple comparison procedures with each treatment serving as independent variables.

3. Results

3.1. Ae. aegypti and other mosquitoes encode only one neuroparsin gene

The Pfam database describes neuroparsins (PF07327) as a protein family from arthropods that consists of neuropeptides (103-201 amino acids) with pleiotrophic activities. A BLAST search of the *Ae. aegypti* genome using OEH indicated that the only neuroparsin

gene present was OEH itself. Likewise, only one neuroparsin gene was identified in the genomes of *C. quinquefasciatus* and *An. gambiae*. These findings were similar to those reported by Veenstra (2010), who noted that several *Drosophila* species also encode only one neuroparsin gene, although members of the *D. melanogaster* subgroup encode no recognizable neuroparsin. Given these findings and recent comparative studies showing that OEH function in mosquitoes is likely conserved (Gulia-Nuss et al., 2012), we hereafter referred to the dipteran neuroparsins as OEHs. Outside of *Ae. aegypti*, data on neuroparsin function and expression are restricted to the orthopterans, *L. migratoria* and *S. gregaria* (Schoofs et al., 1997; Badisco et al., 2007, 2011). Aligning the dipteran OEHs with *L. migratoria* neuroparsin A (NPA) and *S. gregaria* NP1 indicated their most conserved feature was the spacing pattern of eleven cysteine residues (Fig. 1A). Overall sequence similarity to *Ae. aegypti* OEH, however, was relatively low, ranging from 74.5% for *C. quinquefasciatus* OEH to 27% for *S. gregaria* NP1 and 23% for *Drosophila pseudoobscura* OEH (Fig. 1A). Inclusion of the N-terminal domain of human IGFBP7 in this alignment revealed some parallels in cysteine spacing pattern as noted previously (Badisco et al., 2007), but overall similarity to *Ae. aegypti* pre-proOEH was again low (24%) (Fig. 1A).

3.2. Ae. aegypti hemolymph predominantly contains sOEH

Sequence analysis also indicated that *Ae. aegypti* lOEH contained a basic amino acid (arginine) at residue 108 corresponding to the C-terminus of sOEH, and that similarly positioned mono- or dibasic sites were present in other predicted dipteran OEHs (Fig. 1A). Correspondingly, immunoblot analysis of protein extracts prepared from *Ae. aegypti* adult female heads showed that anti-OEH predominantly detected a band with a mass similar to the predicted size of lOEH in protein extracts prepared from *Ae. aegypti* adult female heads. In contrast, anti-OEH predominantly detected a band with a mass similar to the predicted size of sOEH in hemolymph (Fig. 1B).

3.3. rlOEH, sOEH and ILP3 exhibit similar biological activity

Prior studies showed that sOEH and ILP3 dose-dependently stimulate yolk deposition into oocytes and ECD production by ovaries at similar concentrations (0.1–10 pmol) (Brown et al., 1998, 2008). In contrast, no functional studies had been conducted with lOEH. We therefore compared the biological activity of rlOEH to sOEH and ILP3. *In vivo* yolk deposition assays measured at 24 and 48 h PBM showed that rlOEH and ILP3 stimulated a stronger yolk deposition response than sOEH at the lowest dose tested (0.2 pmol), but at higher doses each peptide stimulated a similar or only slightly lower response than found for intact (i.e. non-decapitated), blood-fed females which served as our positive control (Fig. 2). In our *in vitro* ECD assays, we compared the activity of each peptide in saline or Sf-900 medium, because prior studies had shown that ovaries responded more strongly to ILP3 when amino acids were present (Gulia-Nuss et al., 2011). In saline, sOEH, rlOEH and ILP3 did not increase ECD production at the lowest dose tested (0.1 pmol) relative to our negative control (saline only), but each peptide significantly increased ECD production at a dose of 5 pmol or more (Fig. 3A). In Sf-900 medium, ILP3 significantly increased ECD production relative to the negative control (medium only) at all doses tested, whereas sOEH and rlOEH significantly increased ECD production at a dose of 5 pmol or more (Fig. 3B).

As previously reported (Gulia-Nuss et al., 2011), ovaries stimulated with a given dose of ILP3 produced more ECD in Sf-900 medium than saline (Fig. 3). sOEH and rlOEH exhibited the same trend, which suggested that the activity of both ILP3 and OEH is coupled
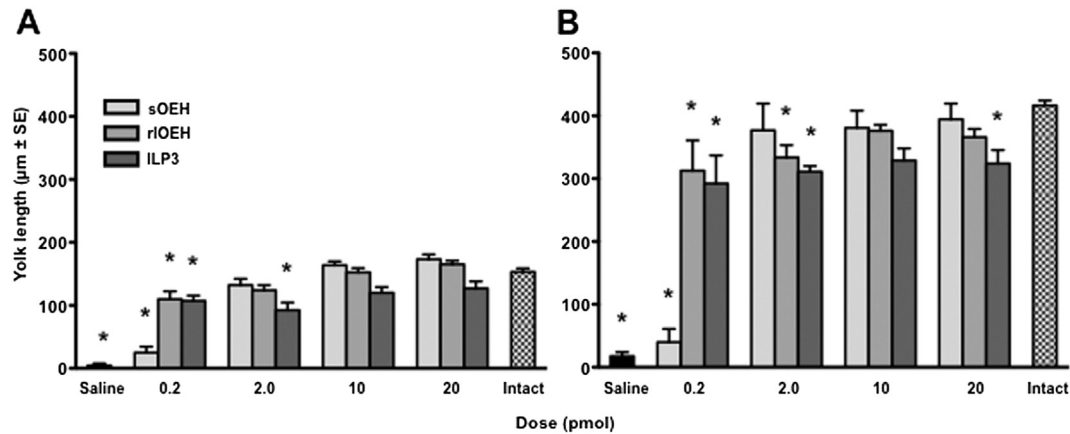
Fig. 2. rlOEH and sOEH dose-dependently stimulate yolk deposition into oocytes. Adult female *Ae. aegypti* were decapitated 1 h PBM and injected with 0.2—20 pmol of rlOEH, sOEH, or ILP3 followed by dissection and measurement of yolk deposition as determined by oocyte length (mean ± SE) at 24 (A) or 48 h (B) PBM. Decapitated females injected with saline only served as a negative control while intact (non-decapitated) females served as a positive control. Yolk deposition increases with dose of each peptide at 24 h ($F_{13, 199} = 30.2$, $P < 0.0001$) and 48 h ($F_{13, 167} = 32.6$, $P < 0.0001$) PBM. Asterisks above bars in each graph indicate means that significantly differ from the positive control (Dunnett's comparison of means with control, $\alpha = 0.05$).

with amino acid sensing through the TOR pathway. Repeating the rlOEH assays in the presence or absence of the TOR complex 1 (TORC1) inhibitor rapamycin supported this suggestion by showing that ECD production in Sf-900 medium was reduced to similar levels observed when ovaries were incubated in saline (Fig. 4). In sum, these data indicated that rlOEH and sOEH exhibit similar gonadotropic activity *in vivo* and *in vitro*, which is enhanced by the presence of amino acids.

3.4. rlOEH activity does not depend on binding to ILP3 or the MIR

We previously reported that anti-ILP binds ILP3 (Brown et al., 2008), while results presented above show that anti-OEH recognizes lOEH and sOEH. We therefore used an immunoprecipitation approach to assess whether purified rlOEH or sOEH bound to ILP3 in solution. We observed that anti-OEH and anti-ILP3 captured rlOEH, sOEH and ILP3 when these peptides were alone or together in solution, but we never detected co-immunoprecipitation of ILP3 by anti-OEH or either OEH by anti-ILP3 (data not presented). We also used radiolabeled ILP3 and ILP4 and a cross-linking approach to detect a binding interaction. In these experiments, we consistently detected a 6 kDa band on autoradiographs that corresponded

to the mass of ILP3 but we never observed a higher molecular mass conjugate indicative of OEH-ILP3 binding (Supplementary Fig. 1). Finally, we assessed whether OEH might bind to the MIR itself using ovary membranes and conditions optimized previously for high affinity binding of ILP3 to the MIR (Wen et al., 2010). However, no binding of radiolabeled rlOEH or sOEH to the MIR was detected (data not presented). We thus concluded that OEH does not directly bind to ILP3 or the MIR.

ILP3 activity fully depends on binding to the MIR and knockdown of the MIR by RNA interference (RNAi) greatly reduces ILP3-mediated yolk uptake and ECD production (Brown et al., 2008; Wen et al., 2010; Gulia-Nuss et al., 2011). To assess whether OEH activity indirectly required the MIR, we measured ECD production by ovaries in Sf-900 medium containing PQIP, which is a potent and specific inhibitor that blocks ligand induced activation of the mammalian IR and insulin-like growth factor 1 receptor (IGF-1R) (Ji et al., 2007; Flanigan et al., 2010). No studies to our knowledge had previously assessed whether PQIP similarly inhibits activation of an insect IR. We therefore first conducted dose response studies that assessed whether PQIP disabled ILP3 activity using our *in vitro* ECD assay. Using 10 pmol of ILP3, we determined that 50 pmol of PQIP had no inhibitory effect on ECD production by ovaries but 5 nmol or
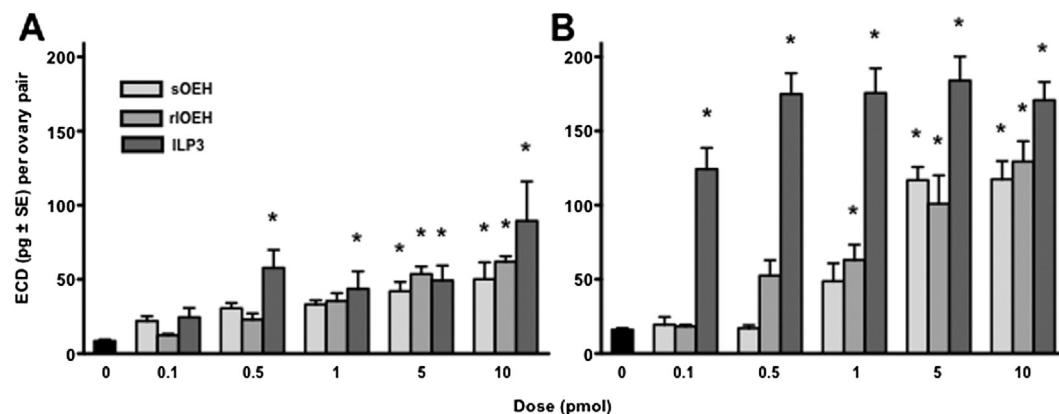
Fig. 3. rlOEH and sOEH dose-dependently stimulate ECD production by ovaries. Ovaries from non-blood fed females were incubated in saline (A) or Sf-900 medium (B) plus 0.1—10 pmol of rlOEH, sOEH, or ILP3 for 6 h followed by measurement of secreted ECD by radioimmunoassay. Ovaries incubated in saline or medium without peptide (0) served as the control. ECD production increases with dose of each peptide in saline ($F_{15, 95} = 6.5$, $P < 0.0001$) and Sf-900 medium ($F_{15, 119} = 29.8$, $P < 0.0001$). Asterisks above bars indicate means that significantly differ from the control (Dunnett's comparison of means with control, $\alpha = 0.05$).
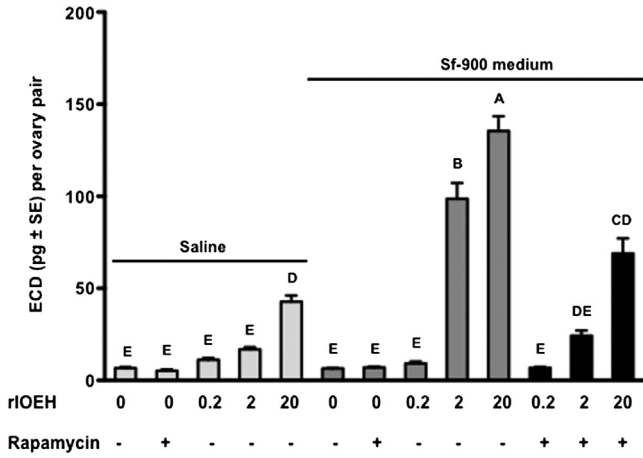
Fig. 4. Rapamycin reduces rlOEH-stimulated production of ECD by ovaries in Sf-900 medium to similar levels produced in saline. Ovaries from non-blood fed females were incubated in saline or Sf-900 medium for 6 h in the presence or absence of rlOEH (0—20 pmol) and rapamycin (100 pmol). Secreted ECD (mean ± SE) was measured by radioimmunoassay. Different letters above bars in the graph indicate means that significantly differ ($F_{12, 166} = 98.3$, $P < 0.0001$) with comparisons of all pairs performed using the Tukey—Kramer multiple comparison procedure ($\alpha = 0.05$).
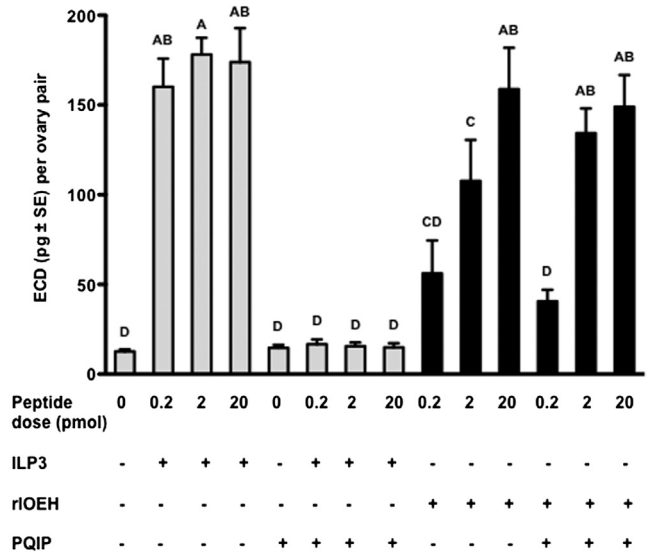
Fig. 5. PQIP inhibits ILP3-stimulated production of ECD but has no effect on rlOEH. Ovaries from non-blood fed females were incubated in Sf-900 medium for 6 h in the presence or absence of ILP3 or rlOEH (0—20 pmol) and PQIP (5 nmol). Secreted ECD (mean ± SE) was measured by radioimmunoassay. Different letters above bars in the graph indicate means that significantly differ ($F_{13, 125} = 25.1$, $P < 0.0001$) with comparisons of all pairs of means performed using the Tukey—Kramer multiple comparison procedure ($\alpha = 0.05$).

more of PQIP reduced ECD production to background levels (data not presented). We thus used 5 nmol of PQIP to compare its effects on the activity of ILP3 and rlOEH. These results showed that PQIP reduced ECD production to background levels when ovaries were stimulated with 0.2—20.0 pmol of ILP3 (Fig. 5). Consistent with the outcome of our binding studies, however, PQIP had no effect on ECD production by ovaries stimulated by rlOEH (Fig. 5).

3.5. lOEH and ILP3 signaling converge downstream of the MIR

Since ILP3 and OEH activity both show evidence of linkage to TOR signaling in ovaries but only ILP3 requires the MIR for function, we examined how the insulin and TOR pathways in ovaries responded to each peptide. Both pathways are conserved across eukaryotes with phosphorylation of Akt (p-Akt) serving as a marker for activation of insulin signaling and phosphorylation of S6K (p-S6K) for activation of TOR signaling (Baker and Thummel, 2007; Grewal, 2009; Fontana et al., 2010; Gaubitz and Loewith, 2012). We thus incubated ovaries from non-blood fed females with rlOEH or ILP3 and then used antibodies that recognize the MIR, p-MIR, p-Akt and p-S6K on immunoblots from ovary extracts to assess activation of each pathway. Given the lack of literature on detecting phosphorylation of these pathway components in mosquito ovaries, we first optimized approaches for sample preparation. Our results showed that each marker protein was best detected when ovaries (20 pairs/treatment) were incubated *in vitro* with 40 pmol of rlOEH or ILP3 for 30 min followed by adding ovary extracts to a 100 kDa spin column filter and immunoblotting the retentate. The value of this simple approach is well illustrated using ILP3 in Sf-900 medium, and antibodies that detect the MIR and p-Akt. As expected, the large, membrane bound MIR (~500 K MW) was strictly present in the retentate from the spin column (Fig. 6). p-Akt with a predicted mass of ca. 55 kDa, however, was also only detected in the retentate presumably due to complex formation by insulin signaling pathway components (Fig. 6).

Using these methods, we first compared the effects of rlOEH and ILP3 when ovaries were incubated in saline. These assays indicated that ILP3 stimulated phosphorylation of the MIR while rlOEH did not (Fig. 7A). In contrast, both neuropeptides stimulated phosphorylation of Akt to comparable levels but did not stimulate
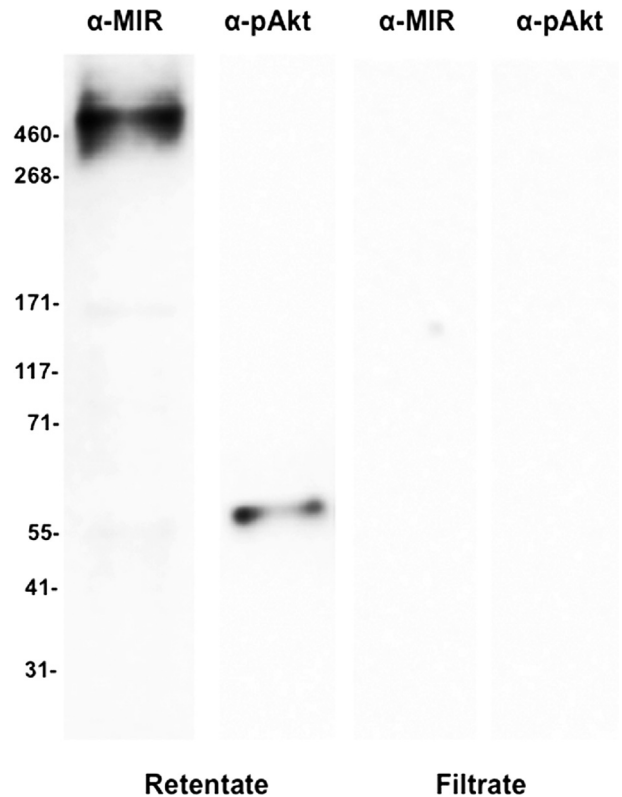
Fig. 6. Immunoblot of total protein ovary extracts prepared after a 30 min incubation with ILP3 (40 pmol). Extracts were then separated on a 100 kDa spin column and probed with antibodies that detect the MIR (α-MIR) or phosphorylated Akt (α-pAkt). Single bands corresponding to the MIR and pAkt are detected in the retentate but no proteins are detected in the filtrate. Molecular mass markers are indicated to the left of the blot.

phosphorylation of S6K (Fig. 7A). We also noted that no phosphorylation of Akt or S6K was detectable in control samples lacking ILP3 or rlOEH (Fig. 7A). We then conducted the same experiments in Sf-900 medium in the presence and absence of PQIP or rapamycin. ILP3 stimulated phosphorylation of the MIR, Akt and S6K with PQIP blocking phosphorylation of each marker, and rapamycin only blocking phosphorylation of S6K (Fig. 7B). rlOEH in contrast did not stimulate phosphorylation of the MIR, but it did stimulate phosphorylation of Akt and S6K. Rapamycin, as expected, blocked phosphorylation of S6K stimulated by rlOEH, but PQIP had no effect on rlOEH-mediated phosphorylation of Akt or S6K (Fig. 7B). These data also showed that none of the marker proteins including S6K were phosphorylated in the control sample despite the presence of amino acids in the culture medium (Fig. 7B). Taken together, these experiments showed that PQIP inhibits phosphorylation of the MIR and activation of the insulin signaling pathway by ILP3, whereas rlOEH activates Akt independently of MIR activation. These data also strongly suggested that TOR activity in the mosquito ovary requires activation of the insulin signaling pathway by either ILP3 or rlOEH.

4. Discussion

It has long been known that blood feeding stimulates the release of ILPs and OEH from medial neurosecretory cells in the brain of *Ae. aegypti* females, and that both directly stimulate ovaries to produce ECD, which activates yolk production and uptake by oocytes (Brown et al., 1998, 2008; Gulia-Nuss et al., 2011; Riddiford, 2013). Prior studies also show that ILP3 activates insulin signaling through binding to the MIR in ovaries (Brown et al., 2008; Wen et al., 2010). In contrast, the role of OEH in mosquito reproduction has remained unclear because almost nothing is known about its mode of action.

Vertebrate IGFBPs negatively or positively modulate the activity of IGFs by altering binding to IGFRs (Mohan and Baylink, 2002; Rosenzweig and Atreya, 2010). Claeys et al. (2003) were the first to suggest that neuroparsins share features with the N-terminal domain of vertebrate IGFBPs, which led to the hypothesis that neuroparsin functions by binding to ILPs (Badisco et al., 2007). A subsequent study presented dot blots showing that recombinant neuroparsin bound ILP isolated from *S. gregaria* (Badisco et al., 2008). On the other hand, vertebrate IGFBPs are larger proteins (22–31 kDa) than neuroparsins, and their ability to bind IGFs involves residues in both their N- and C-terminal domains (Rosenzweig and Atreya, 2010). Veenstra (2010) further noted that overall similarities between neuroparsins and IGFBPs are weak, and that arthropods encode other proteins that structurally and functionally appear to be IGFBP homologs. These findings together with the observation that neuroparsins are produced in neuroendocrine cells but IGFBPs are not, also led Veenstra (2010) to conclude that neuroparsins likely do not function as ILP binding proteins.

In the first part of this study, we compared neuroparsin family members from mosquitoes, *Drosophila* and orthopterans to assess gene diversity and look for features associated with potential processing of lOEH to sOEH. Similar to *Drosophila* sp. outside the *D. melanogaster* subgroup (Veenstra, 2010), these data show that mosquitoes encode only one neuroparsin gene, which in *Ae. aegypti* produces only one transcript (Brown et al., 1998). These diverse insect neuroparsins share similar patterns in cysteine spacing but overall sequence similarity is variable. Despite differences in primary sequence, however, comparative studies show that rlOEH from *Ae. aegypti* has very similar biological activity in two other mosquitoes, *Georgecraigius atropalpus* (Gulia-Nuss et al., 2012) and *An. gambiae* (Brown, M. R. and Strand, M. R., unpublished), which suggests OEH function in mosquito reproduction is likely conserved. Neuroparsins from hemimetabolous insects in contrast
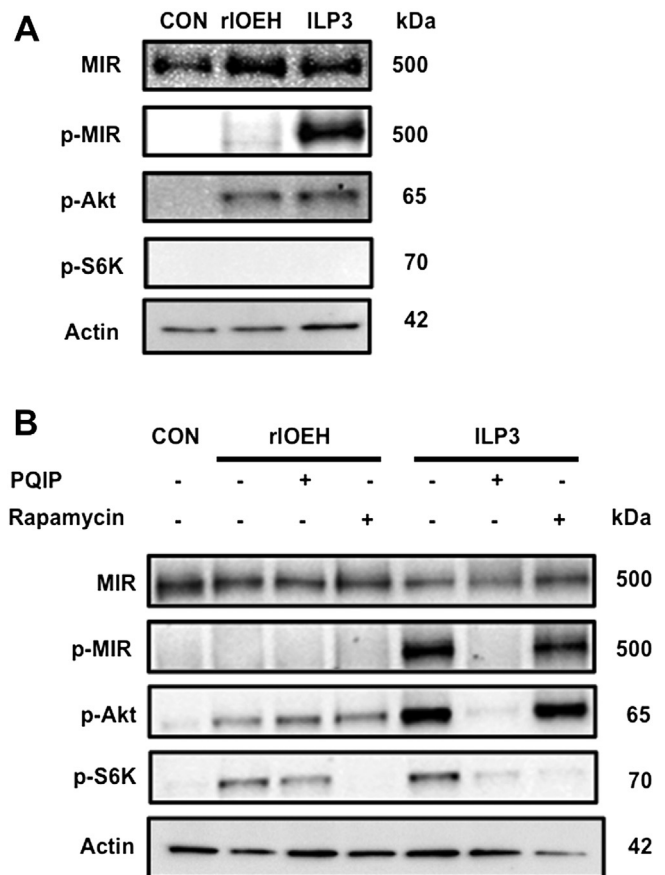
Fig. 7. rlOEH activates Akt but not the MIR. (A) Signaling protein activation in ovaries incubated in saline. Total protein extracts from saline only control ovaries (CON), and ovaries stimulated with rlOEH or ILP3 for 30 min were processed and probed with antibodies that detect the MIR, phosphorylated MIR (p-MIR), phosphorylated Akt (p-Akt), phosphorylated S6K (p-S6K) or actin which served as a loading control. (B) Signaling protein activation in ovaries incubated in Sf-900 medium. Ovaries were incubated for 30 min in medium only (CON) or medium plus rlOEH or ILP3 with (+) and without (−) PQIP or rapamycin. Samples were then processed and probed as in (A). Only ILP3 elevates p-MIR levels, whereas rlOEH and ILP3 comparably elevate p-S6K. Elevation of p-Akt levels in contrast are higher in response to ILP3 than rlOEH.

exhibit a diversity of functional activities, which could be due to production of different products through alternative splicing (locusts) or the presence of multiple neuroparsin genes (*Rhodnius*) (Claeys et al., 2006; Badisco et al., 2007; Veenstra, 2010).

The detection of sOEH as the predominant form in hemolymph suggests an unknown enzyme processes lOEH to sOEH at a C-terminal monobasic cut site. This finding is consistent with the original purification of sOEH from *Ae. aegypti*, and studies of *G. atropalpus*, which show that its endogenous lOEH is also processed to sOEH (Brown et al., 1998; Gulia-Nuss et al., 2012). The functional significance of processing, however, remains unclear given our results showing *Ae. aegypti* rlOEH and sOEH exhibit very similar biological activity. In contrast, our results provide three lines of evidence that OEH function does not involve binding to ILP3 or activation of the MIR. First, we detect no binding interactions between OEH and ILP3/ILP4 or between OEH and the MIR in our immunoprecipitation, cross-linking, and receptor binding assays. Second, our results indicate that PQIP dose-dependently inhibits ILP3 activity but has no effect on rlOEH. Third, our results clearly show that ILP3 stimulates MIR phosphorylation, which PQIP inhibits, but rlOEH does not. In contrast, our signaling experiments indicate that ILP3 and rlOEH both activate Akt in ovaries. We recognize that mosquitoes and other insects encode multiple ILPs,

which leaves open the possibility that OEH could interact with other ILP family members. However, in light of the binding studies we did conduct together with the overlapping functional activities ILP3 and OEH exhibit, our data much more strongly suggest that OEH activates the insulin signaling pathway in ovaries independently of the MIR by binding to a different receptor.

Insulin and TORC1 signaling both sense nutrient status but whether the two pathways are functionally linked is unsettled, given that some studies from vertebrates or *D. melanogaster* show activation of TORC1 in response to insulin signaling (Cai et al., 2006; Inoki et al., 2002; Manning et al., 2002; Potter et al., 2002) and others not (Dong and Pan, 2004; Hall et al., 2007; Radimerski et al., 2002). More recently, linkage between the insulin and TOR signaling pathways was shown to occur in the ovaries but not other tissues in *D. melanogaster* (Pallares-Cartes et al., 2012). Linkage also depended on the protein PRAS40, which may be differentially phosphorylated by Akt, TORC1, or other kinases in the ovaries relative to other tissues (Pallares-Cartes et al., 2012). Prior results with *Ae. aegypti* similarly show that amino acids alone activate TOR signaling in the fat body as measured by phosphorylation of S6K (Roy and Raikhel, 2011), whereas this study shows that S6K phosphorylation in the ovaries requires co-stimulation by amino acids and either ILP3 or OEH. Searching the *Ae. aegypti* and *Culex qunquefaciatus* genomes indicates each encodes one PRAS40 homolog (AAEL006792, CPIJ010527), whereas *An. gambiae* may encode two (APAP012282, AGAP006696). We currently have no evidence these PRAS40 homologs are required for coupling of insulin and TOR signaling. However, our results showing that rlOEH and ILP3 both stimulate S6K phosphorylation in the presence of amino acids supports a role for each in activating the insulin signaling pathway, which in turn is involved in activation of TOR and its target S6K. Identification of the OEH receptor will be key to further understanding the function and signaling of this important neuropeptide. Thereafter, studies will also be needed to dissect the pathways that underlie how ILPs and OEH activate ECD production, and whether oocytes uptake yolk in direct or indirect response to these hormones.

Acknowledgments

Appendix A. Supplementary data

Supplementary data related to this article can be found at http://dx.doi.org/10.1016/j.ibmb.2013.09.004.

References

Antonova, Y., Arik, A.J., Moore, W., Riehle, M.R., Brown, M.R., 2012. Insulin-like peptides: structure, signaling, and function. In: Gilbert, L.I. (Ed.), Insect Endocrinology. Elsevier/Academic Press, New York, pp. 63–92.

Attardo, G.M., Hansen, I.A., Raikhel, A.S., 2005. Nutritional regulation of vitellogenesis in mosquitoes: implications for anautogeny. Insect Biochem. Mol. Biol. 35, 661–675.

Badisco, L., Claeys, I., Van Loy, T., Van Hiel, M., Franssens, V., Simonet, G., Vanden Broeck, J., 2007. Neuroparsins, a family of conserved arthropod neuropeptides. Gen. Comp. Endocrinol. 153, 64–71.

Badisco, L., Claeys, I., Van Hiel, M., Clynen, E., Huybrechts, J., Vandermissen, T., Van Soest, S., Vanden Bosch, L., Simonet, G., Vanden Broeck, J., 2008. Purification and characterization of an insulin-like peptide in the desert locust, *Schistocera gregaria*: immunolocalization, cDNA cloning, transcript profiling, and interaction with neuroparsin. J. Mol. Endocrinol. 40, 137–150.

Badisco, L., Ott, S.R., Rogers, S.M., Matheson, T., Knapen, D., Vergauwen, L., Verlinden, H., Marchal, E., Sheehy, M.R., Burrows, M., Vanden Broeck, J., 2011. Microarray-based transcriptomic analysis of differences between long-term gregarious and solitarious desert locusts. PLoS One 6, e28110.

Baker, K.D., Thummel, C.S., 2007. Diabetic larvae and obese flies-emerging studies of metabolism in *Drosophila*. Cell Metab. 6, 257–266.

Barlos, K., Gatos, D., Kallitsis, J., Papaphotiu, G., Sotiriu, P., Wenqing, Y., Schäfer, W., 1989. Darstellung geschützter Peptid-Fragmente unter Einsatz substituierter Triphenylmethyl-Harze. Tetrahedron 30, 3943–3946.

Barlos, K., Gatos, D., Papaphotiu, G., Schäfer, W., 1993. Synthese von Calcitonin-Derivaten durch Fragmentkondensation in Lösung und am 2-Chlortrityl-Harz. Liebigs Ann. Chem. 1993, 215–220.

Brown, M.R., Cao, C., 2001. Distribution of ovary ecdysteroidogenic hormone I in the nervous system and gut of mosquitoes. J. Insect Sci. 1, 3.

Brown, M.R., Graf, R., Swiderek, K.M., Fendley, D., Stracker, T.H., Champagne, D.E., Lea, A.O., 1998. Identification of a steroidogenic neurohormone in female mosquitoes. J. Biol. Chem. 273, 3967–3971.

Brown, M.R., Clark, K.D., Gulia, M., Zhao, Z., Garczynski, S.F., Crim, J.W., Suderman, R.J., Strand, M.R., 2008. An insulin-like peptide regulates egg maturation and metabolism in the mosquito *Aedes aegypti*. Proc. Natl. Acad. Sci. U. S. A. 105, 5716–5721.

Bryant, B., Macdonald, W., Raikhel, A.S., 2010. microRNA miR-275 is indispensable for blood digestion and egg development in the mosquito *Aedes aegypti*. Proc. Natl. Acad. Sci. U. S. A. 107, 22391–22398.

Cai, S.L., Tee, A.R., Short, J.D., Bergeron, J.M., Kim, J., Shen, J., Guo, R., Johnson, C.L., Kiguchi, K., Walker, C.L., 2006. Activity of TSC2 is inhibited by AKT-mediated phosphorylation and membrane partitioning. J. Cell. Biol. 173, 279–289.

Claeys, I., Simonet, G., Van Loy, T., De Loof, A., Vanden Broeck, J., 2003. cDNA cloning and transcript distribution of two novel members of the neuroparsin family in the desert locust, *Schistocerca gregaria*. Insect Mol. Biol. 12, 473–481.

Claeys, I., Breugelmans, B., Simonet, G., Van Soest, S., Sas, F., De Loof, A., Vanden Broeck, J., 2006. Neuroparsin transcripts as molecular markers in the process of desert locust (*Schistocerca gregaria*) phase transition. Biochem. Biophys. Res. Commun. 341, 599–606.

Clifton, M.E., Noriega, F.G., 2011. Nutrient limitation results in juvenile hormone-mediated resorption of previtellogenic ovarian follicles in mosquitoes. J. Insect Physiol. 57, 1274–1281.

Crim, J.W., Garczynski, S.F., Brown, M.R., 2002. Approaches to radioiodination of insect peptides. Peptides 23, 2045–2051.

Pan, D., Dong, J., Zhang, Y., Gao, X., 2004. Tuberous sclerosis complex: from *Drosophila* to human disease. Trends Cell Biol. 14, 78–85.

Flanigan, S.A., Pitts, T.M., Eckhardt, S.G., Tentler, J.J., Tan, A.C., Thorburn, A., Leong, S., 2010. The insulin-like growth factor I receptor/insulin receptor tyrosine kinase inhibitor PQIP exhibits enhanced antitumor effects in combination with chemotherapy against colorectal cancer models. Clin. Cancer Res. 16, 5436–5446.

Fontana, L., Partridge, L., Longo, V.D., 2010. Extending healthy life span–from yeast to humans. Science 328, 321–326.

Gaubitz, C., Loewith, R., 2012. Amino acid signaling in high definition. Structure 20, 1993–1994.

Grewal, S.S., 2009. Insulin/TOR signaling in growth and homeostasis: a view from the fly world. Int. J. Biochem. Cell Biol. 41, 1006–1010.

Gulia-Nuss, M., Robertson, A.E., Brown, M.R., Strand, M.R., 2011. Insulin-like peptides and the target of rapamycin pathway coordinately regulate blood digestion and egg maturation in the mosquito *Aedes aegypti*. PLoS One 6, e20401.

Gulia-Nuss, M., Eum, J.-H., Strand, M.R., Brown, M.R., 2012. Ovary ecdysteroidogenic hormone activates egg maturation in the mosquito, *Georgecraigius atropalpus*, after adult eclosion or a blood meal. J. Exp. Biol. 215, 3758–3767.

Hall, D.J., Grewal, S.S., de la Cruz, A.F., Edgar, B.A., 2007. Rheb-TOR signaling promotes protein synthesis, but not glucose or amino acid import, in *Drosophila*. BMC Biol. 5, 10.

Han, S.K., Lee, B.I., Cho, W., 1997. Bacterial expression and characterization of human pancreatic phospholipase A2. Biochim. Biophys. Acta 1346, 185–192.

Hansen, I.A., Attardo, G.M., Park, J.H., Peng, Q., Raikhel, A.S., 2004. Target of rapamycin-mediated amino acid signaling in mosquito anautogeny. Proc. Natl. Acad. Sci. U. S. A. 101, 10626–10631.

Hansen, I.A., Attardo, G.M., Roy, S.G., Raikhel, A.S., 2005. Target of rapamycin-dependent activation of S6 kinase is a central step in the transduction of nutritional signals during egg development in a mosquito. J. Biol. Chem. 280, 20565–20572.

Hsih, M.H., Kuo, J.C., Tsai, H.J., 1997. Optimization of the solubilization and renaturation of fish growth hormone produced by *Escherichia coli*. Appl. Microbiol. Biotechnol. 48, 66–72.

Inoki, K., Li, Y., Zhu, t., Wu, J., Guan, K.L., 2002. TSC2 is phosphorylated and inhibited by Akt and suppresses mTOR signaling. Nat. Cell Biol. 4, 648–657.

Ji, Q.S., Mulvihill, M.J., Rosenfeld-Franklin, M., Cooke, A., Feng, L., Mak, G., O'Connor, M., Yao, Y., Pirritt, C., Buck, E., Eyzaguirre, A., Arnold, L.D., Gibson, N.W., Pachter, J.A., 2007. A novel, potent, and selective insulin-like growth factor-I receptor kinase inhibitor blocks insulin-like growth factor-I receptor signaling in vitro and inhibits insulin-like growth factor-I receptor dependent tumor growth in vivo. Mol. Cancer Ther. 6, 2158–2167.

Katoh, K., Kuma, K., Toh, H., Miyata, T., 2005. MAFFT version 5: improvement in accuracy of multiple sequence alignment. Nucleic Acids Res. 33, 511–518.

Magnuson, B., Ekim, B., Fingar, D.C., 2012. Regulation and function of ribosomal protein S6 kinase (S6K) within mTOR signalling networks. Biochem. J. 441, 1–21.

Manning, B.D., Tee, A.R., Logsdon, M.N., Blenis, J., Cantley, L.C., 2002. Identification of the tuberous sclerosis complex-2 tumor suppressor gene product tuberin as a target of the phosphoinositide 3-kinase/akt pathway. Mol. Cell 10, 151–162.

Matsumoto, S., Brown, M.R., Lea, A.O., Suzuki, A., 1989. Isolation and characterization of ovarian ecdysteriodogenic hormones from the mosquito, Aedes aegypti. Insect Biochem. 19, 651–656.

Mohan, S., Baylink, D.J., 2002. IGF-binding proteins are multifunctional and act via IGF-dependent and -independent mechanisms. J. Endocrinol. 175, 19–31.

Pallares-Cartes, C., Cakan-Akdogan, G., Teleman, A.A., 2012. Tissue-specific coupling between insulin/IGF and TORC1 signaling via PRAS40 in Drosophila. Dev. Cell. 22, 172–182.

Pérez-Hedo, M., Rivera-Perez, C., Noriega, F.G., 2013. The insulin/TOR signal transduction pathway is involved in the nutritional regulation of juvenile hormone synthesis in Aedes aegypti. Insect Biochem. Mol. Biol. 43, 495–500.

Potter, C.J., Pedraza, L.G., Xu, T., 2002. Akt regulates growth by directly phosphorylating Tsc2. Nat. Cell Biol. 4, 658–665.

Radimerski, T., Montagne, J., Rintelen, F., Stocker, H., van der Kaay, J., Downes, C.P., Hafen, E., Thomas, G., 2002. dS6K-regulated cell growth is dPKB/dPI(3)K-independent, but requires dPDK1. Nat. Cell Biol. 4, 251–255.

Riddiford, L.M., 2013. Microarrays reveal discrete phases in juvenile hormone regulation of mosquito reproduction. Proc. Natl. Acad. Sci. U. S. A. 110, 9623–9624.

Riehle, M.A., Fan, Y., Cao, C., Brown, M.R., 2006. Molecular characterization and developmental expression of insulin-like peptides in the yellow fever mosquito, Aedes aegypti: expression, cellular localization, and phylogeny. Peptides 27, 2547–2560.

Rosenzweig, S.A., Atreya, H.S., 2010. Defining the pathway to insulin-like growth factor system targeting in cancer. Biochem. Pharmacol. 80, 1115–1124.

Roy, S.G., Raikhel, A.S., 2011. The small GTPase Rheb is a key component linking amino acid signaling and TOR in the nutritional pathway that controls mosquito egg development. Insect Biochem. Mol. Biol. 41, 62–69.

Roy, S.G., Hansen, I.A., Raikhel, A.S., 2007. Effect of insulin and 20-hydroxyecdysone in the fat body of the yellow fever mosquito, Aedes aegypti. Insect Biochem. Mol. Biol. 37, 1317–1326.

Schoofs, L., Veelaert, D., Vanden Broeck, J., De Loof, A., 1997. Peptides in the locusts, Locusta migratoria and Schistocerca gregaria. Peptides 18, 145–156.

Sieglaff, D.H., Duncan, K.A., Brown, M.R., 2005. Expression of genes encoding proteins involved in ecdysteroidogenesis in the female mosquito, Aedes aegypti. Insect Biochem. Mol. Biol. 35, 369–514.

Veenstra, J.A., 2010. What the loss of the hormone neuroparsin in the melanogaster subgroup of Drosophila can tell us about its function. Insect Biochem. Mol. Biol. 40, 354–361.

Wen, Z., Gulia, M., Clark, K.D., Dhara, A., Crim, J.W., Strand, M.R., Brown, M.R., 2010. Two insulin-like peptide family members from the mosquito Aedes aegypti exhibit differential biological and receptor binding activities. Mol. Cell. Endocrinol. 328, 47–55.

Wu, Q., Brown, M.R., 2006. Signaling and function of insulin-like peptides in insects. Ann. Rev. Entomol. 51, 1–24.

Zhu, J., Chen, L., Raikhel, A.S., 2003. Posttranscriptional control of the competence factor betaFTZ-F1 by juvenile hormone in the mosquito Aedes aegypti. Proc. Natl. Acad. Sci. U. S. A. 100, 13338–13343.

Zhu, J., Chen, L., Sun, G., Raikhel, A.S., 2006. The competence factor beta Ftz-F1 potentiates ecdysone receptor activity via recruiting a p160/SRC coactivator. Mol. Cell. Biol. 26, 9402–9412.

Zou, Z., Saha, T.T., Roy, S., Shin, S.W., Backman, T.W., Girke, T., White, K.P., Raikhel, A.S., 2013. Juvenile hormone and its receptor, methoprene-tolerant, control the dynamics of mosquito gene expression. Proc. Natl. Acad. Sci. U. S. A. 110, 2173–2181.